Long-wavelength optic vibrations in a superlattice

Kun Huang
Institute of Semiconductors, Chinese Academy of Sciences, Beijing, China

Bang-Fen Zhu*
Center of Theoretical Physics, Chinese Center of Advanced Science and Technology (World Laboratory), Beijing, China and Institute of Semiconductors, Chinese Academy of Sciences, Beijing, China

(Received 2 February 1988)

For a critical examination of the dielectric continuum model as applied to a superlattice, we have introduced a microscopic model, which takes proper account of the long-range Coulomb interaction and yet permits easy solution for the long-wavelength LO and TO modes. With this model, it is shown that such long-wavelength modes approach different limits depending on directions of propagation relative to the axis of the superlattice. This demonstrates that to treat the confined bulklike modes in superlattices as modes of isolated slabs is inadequate.

According to the dielectric continuum theory,[1-3] the optic modes in a superlattice consist of bulklike modes confined to slabs of either constituent material and certain interface modes. In this theory, the bulklike modes confined to different slabs are completely decoupled. Thus the early treatment of lattice vibrations of a slab of ionic crystal by Fuchs and Kliewer[4] has become a standard reference in discussion of the optic modes in superlattices. The vibration modes derived from Raman scattering are directly identified with the slab modes.[5-7] As slabs have translational symmetry only parallel to the slab plane, only the parallel component $\mathbf{k}_\parallel$ of the phonon vector $\mathbf{k}$ is considered as effective.[7] Thus a long-wavelength phonon such as observed in Raman scattering, no matter in what direction its wave-number vector lies, is identified with a $\mathbf{k}_\parallel \to \mathbf{0}$ mode. In the following, we shall show by a simple model that long-wavelength optic modes with $\mathbf{k}$ differently oriented with respect to the axis of a superlattice are clearly distinct and converge to different limits when $\mathbf{k} \to \mathbf{0}$.

Our basic approach is to work out a microscopic model for an $AB\,AB\,AB\ldots$ superlattice, which is completely compatible with the dielectric continuum model in the long-wavelength limit (i.e., with respect to bulk A and B materials) and takes proper account of the long-range Coulomb interaction. Moreover, it should be simple so as to permit rigorous and definitive conclusions to be drawn about long-wavelength optic modes with differently oriented wave-number vectors. Thus we use a model in which we simulate the relative motion of the oppositely charged particles in the lattice cell by a charged oscillator. We first consider the A material to be modeled by a simple cubic lattice of oscillators, associated with corresponding electric dipoles. Then the $AB\,AB\,AB\ldots$ superlattice can be envisaged as formed as follows: along a cubic axis (to become the axis of the superlattice and designated as the z axis) of the A lattice, after every m layer (in the xy plane) of A oscillators, follow m layers of B oscillators, which differ only in a change of the intrinsic oscillator frequency ω_0 to be expressed in terms of

$$\Delta\omega_0^2=\omega_0^2(B)-\omega_0^2(A)\ . \tag{1}$$

While the model in itself can contain the full play of the Coulomb interaction and yet circumvents the difficulty of directly dealing with the long-range Coulomb interaction in a superlattice, it clearly has its formal limitations. Thus the model implies that the two materials have the same bulk phonon dispersions apart from a rigid shift of $\Delta\omega_0^2$. However, as the calculated optic models are mainly confined to one of the materials, one can use the dispersion parameters of the material to which the calculated modes are confined. The situation is somewhat similar to the usual effective-mass treatment of quantum-well electrons, where the barrier material is effectively assumed to have the same effective masses as the well material. The important parameter is the barrier height; $\Delta\omega_0^2$ here is just its equivalent.

To work out the vibrational modes of this model superlattice, we can think of (1) as an added "perturbation" (not implying it being small) on the simple A lattice, which owing to its superlattice periodicity of $2ma$ (a is the lattice constant) will couple together the A lattice modes,

$$\frac{1}{N^{3/2}}e^{i\mathbf{k}_s\cdot\mathbf{R}_n}\mathbf{u}\begin{bmatrix}\mathbf{k}_s\\ j\end{bmatrix}\quad (j=1,2,3)\ , \tag{2}$$

with wave-number vectors $\mathbf{k}_s$ related by reciprocal-lattice vectors of the superlattice, which can be expressed as follows:

$$\begin{aligned}\mathbf{k}_s&=\mathbf{k}+\left[\frac{s\pi}{ma}\right]\hat{\mathbf{z}}\\ &=\left[\mathbf{k}_\parallel,k_z+\left[\frac{s\pi}{ma}\right]\right]\end{aligned} \tag{3}$$

($\hat{\mathbf{x}}$, $\hat{\mathbf{y}}$, and $\hat{\mathbf{z}}$ are unit vectors along the cubic axes), where

$$s=-m,-(m-1),\ldots 0,\ldots,(m-2),(m-1) \quad (4)$$

and k_z is restricted to the minizone

$$-\frac{\pi}{2ma}<k_z<\frac{\pi}{2ma} . \quad (5)$$

Owing to the superlattice periodicity, the lattice modes are to be specified by a wave-number vector $\mathbf{k}$ ($\mathbf{k}_{\parallel},k_z$). Clearly we can conveniently work out the lattice modes with wave-number vector $\mathbf{k}$ of the superlattice by using the above A lattice modes as the basis vectors. With these basic vectors, one readily deduces the corresponding dynamical matrix:

$$\langle \mathbf{k}_{s'}j' \mid H \mid \mathbf{k}_s j\rangle=\delta_{ss'}\delta_{jj'}(\omega^2(k_s j)+\tfrac{1}{2}\Delta\omega_0^2) + \left[\frac{\sin(s-s')\pi/2}{\sin(s-s')\pi/2m}\right]\frac{\Delta\omega_0^2}{2m} \times \mathbf{u}(\mathbf{k}_{s'}j')\cdot\mathbf{u}(k_s j)(1-\delta_{ss'}) , \quad (6)$$

where $\omega^2(\mathbf{k}_s j)$ are the squared frequencies of the A lattice modes.

For the purpose of the present Brief Report, we shall specifically discuss only the long-wavelength modes with

$$k \ll \pi/ma . \quad (7)$$

The dynamical matrix (6) is particularly simple with such long-wavelength modes, because for all wave-number vectors $\mathbf{k}_s$ with $s\neq 0$, we can simply put

$$\mathbf{k}_s=\mathbf{k}+\frac{s\pi}{ma}\hat{\mathbf{z}}=\frac{s\pi}{ma}\hat{\mathbf{z}} \quad (s\neq 0) . \quad (8)$$

These $s\neq 0$ modes, which we shall designate simply as the s modes, are essentially independent of the wave-number vector of the long-wavelength mode. They all represent modes along the z axis and owing to the cubic symmetry are either longitudinal, polarized along the z axis,

$$\mathbf{u}\begin{bmatrix} s \\ 3 \end{bmatrix}=\hat{\mathbf{z}}$$

with frequencies which we denote by

$$\omega_{\mathrm{LO}}(s) , \quad (9)$$

or transverse, polarized in the xy plane,

$$\mathbf{u}\begin{bmatrix} s \\ 1 \end{bmatrix}=\hat{\mathbf{x}}; \quad \mathbf{u}\begin{bmatrix} s \\ 2 \end{bmatrix}=\hat{\mathbf{y}}$$

with frequencies which we denote by

$$\omega_{\mathrm{TO}}(s) . \quad (10)$$

On the other hand, the $s=0$ modes are completely determined by the wave-number vector of the long-wavelength mode:

$$\mathbf{k}_{s=0}=\mathbf{k} . \quad (11)$$

Such long-wavelength modes in a lattice with cubic symmetry as in the present simple A lattice are well known to consist of a longitudinal mode with frequency ω_{LO} and two transverse modes with frequency ω_{TO}.

To obtain some concrete idea of how long-wavelength modes propagating in different directions differ, in the following we examine separately long-wavelength modes propagating along and perpendicular to the axis of the superlattice. We notice that in both these cases the three $s=0$ modes (one LO, two TO) can be taken to be polarized along the x, y, and z axes. As the dynamical matrix (6) does not couple modes with mutually perpendicular polarizations, in both cases the dynamical matrix will resolve into three $2m\times 2m$ matrices, each involving one $s=0$ mode and $2m-1$ s modes, all polarized along one of the cubic axes. Since in these matrices only modes with completely parallel polarizations are coupled, from (6) one sees that the nondiagonal elements do not differ in all these cases and only the diagonal matrix elements differ. Thus for comparison, we list below the diagonal elements of the dynamical matrix for modes polarized in the x, y, and z directions, separately for long-wavelength modes propagating along the z direction (along the axis of the superlattice) and along the y direction (perpendicular to the axis of the superlattice). For long-wavelength modes propagating along the axis of the superlattice $\mathbf{k}$ $(0,0,k_z)$ with x, y, and z polarizations, respectively, they are

$$\omega_{\mathrm{TO}}^2(-m),\ldots,\omega_{\mathrm{TO}}^2(-1),\omega_{\mathrm{TO}}^2,\omega_{\mathrm{TO}}^2(1),\ldots,\omega_{\mathrm{TO}}^2(m-1) ;$$

$$\omega_{\mathrm{TO}}^2(-m),\ldots,\omega_{\mathrm{TO}}^2(-1),\omega_{\mathrm{TO}}^2,\omega_{\mathrm{TO}}^2(1),\ldots,\omega_{\mathrm{TO}}^2(m-1) ;$$

$$\omega_{\mathrm{LO}}^2(-m),\ldots,\omega_{\mathrm{LO}}^2(-1),\omega_{\mathrm{LO}}^2,\omega_{\mathrm{LO}}^2(1),\ldots,\omega_{\mathrm{LO}}^2(m-1) .$$

For long-wavelength modes propagating perpendicular to the axis of the superlattice $\mathbf{k}(0,k_y,0)$ with x, y, and z polarizations, respectively, they are

$$\omega_{\mathrm{TO}}^2(-m),\ldots,\omega_{\mathrm{TO}}^2(-1),\omega_{\mathrm{TO}}^2,\omega_{\mathrm{TO}}^2(1),\ldots,\omega_{\mathrm{TO}}^2(m-1) ;$$

$$\omega_{\mathrm{TO}}^2(-m),\ldots,\omega_{\mathrm{TO}}^2(-1),\omega_{\mathrm{LO}}^2,\omega_{\mathrm{TO}}^2(1),\ldots,\omega_{\mathrm{TO}}^2(m-1) ;$$

$$\omega_{\mathrm{LO}}^2(-m),\ldots,\omega_{\mathrm{LO}}^2(-1),\omega_{\mathrm{TO}}^2,\omega_{\mathrm{LO}}^2(1),\ldots,\omega_{\mathrm{LO}}^2(m-1) .$$

Comparing the two cases, we see that they certainly show a difference, namely, the roles of ω_{LO} and ω_{TO} are interchanged for the y- and z-polarized modes. One may further infer from this that the difference between long-wavelength modes propagating in different directions has its origin in the long-range Coulomb interaction, because, as is well known, the difference between ω_{LO} and ω_{TO} is due to macroscopic fields resulting from long-range Coulomb interactions.

Actual computations of the long-wavelength modes from the dynamical matrix (6) require for input only the dispersion curves for the LO and TO modes of the A lattice along a cubic axis and the parameter $\Delta\omega_0^2$, which expresses the relative shift between the dispersion curves of the A and B lattices (throughout this Brief Report always referring to squared frequencies). We can divide the dynamical matrix (6) by $\Delta\omega_0^2$ and work with dimensionless quantities. For our calculations, the LO and TO

dispersion curves are taken as parabolic:

$$\omega_{\mathrm{LO}}^2(s)=\omega_{\mathrm{LO}}^2-B_{\mathrm{LO}}[k_s/(\pi/a)]^2$$
$$=\omega_{\mathrm{LO}}^2-B_{\mathrm{LO}}(s/m)^2\,, \tag{12}$$
$$\omega_{\mathrm{TO}}^2(s)=\omega_{\mathrm{TO}}^2-B_{\mathrm{TO}}[k_s/(\pi/a)]^2$$
$$=\omega_{\mathrm{TO}}^2-B_{\mathrm{TO}}(s/m)^2\,, \tag{13}$$

where ω_{LO}^2, ω_{TO}^2, B_{LO}, and B_{TO} are all understood to be dimensionless.

We have made calculations with parameters which simulate the phonon dispersions of GaAs for long-wavelength modes propagating in general directions in the yz plane. The results can be summarized as follows.

(a) For long-wavelength modes along the z direction, as the $s=0$ modes have the same direction of propagation and TO,LO polarizations as the s modes, one expects this case to be "normal" and the results close to those of much-discussed linear-chain models. This expectation is confirmed by the calculated results, which show that both the longitudinal (z direction) and the transverse (x,y directions) modes are vibrations confined to either A layers or B layers with $0,1,2,\ldots,m-1$ nodes (internal nodes). As shown in Fig. 1, the column marked "$\theta=0°$" illustrates the vibration patterns of the LO modes confined to A layers with 0, 2, and 4 nodes calculated in a $2m=7+7$ model. One finds that if these confined modes are identified with sinusoidal waves (with the same number of nodes) with nodes at both faces of a slab of a definite thickness d, their frequencies fall accurately on the bulk dispersion curves given in (12) and (13). The thickness d is found to be close to but not exactly equal to ma, which is the thickness of the A and B layers.

(b) Long-wavelength modes along the y direction are found to differ from the above most conspicuously in the zero-node modes. The results of calculations for a $2m=7+7$ model show that the zero-node LO modes confined to A and B layers are similarly shifted downwards to between the corresponding three-node and four-node modes and the vibration patterns are also very much altered. Owing to symmetry reasons, the modes with an odd number of nodes are not affected by the change in the direction of the long-wavelength mode, but the even-node modes are perturbed to different degrees according to their closeness to the shifted zero-node mode. The shifted zero-node LO mode and the perturbed even-node modes confined to the A layer are illustrated in the third column of Fig. 1, which can be compared with similarly confined LO modes illustrated in the first column (long-wavelength along the z axis). The behaviors of the LO modes confined to B layers are entirely similar. For the TO modes, the zero-node modes are shifted upwards, thus further removed from the other TO modes, which are therefore less perturbed.

(c) For long-wavelength modes propagating in a general direction in the yz plane, the $s=0$ LO and TO modes in the yz plane are no longer polarized along the cubic axes. They couple simultaneously with the s modes with z polarization [with LO frequencies $\omega_{\mathrm{LO}}(s)$] and the s modes with y polarization [with the TO frequencies $\omega_{\mathrm{TO}}(s)$], leading to $4m\times 4m$ dynamical matrices. In Fig. 2 the calculated squared frequencies are shown as func-

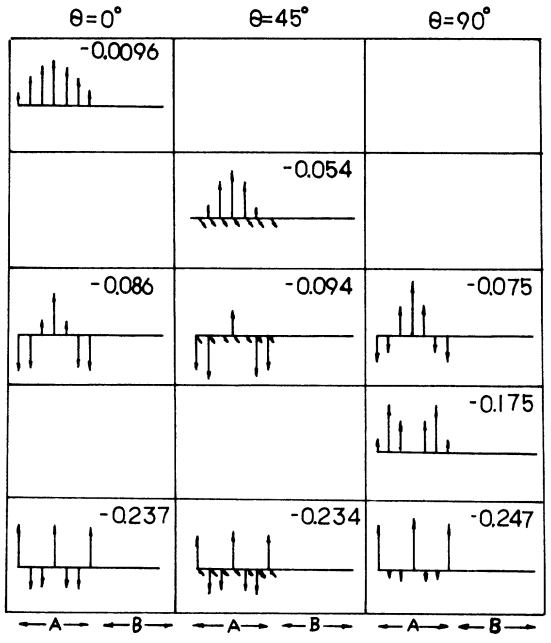

FIG. 1. LO modes for long wavelengths along three directions (the angle θ with the axis of the superlattice $\theta=0°,45°,90°$); vertical and horizontal arrows represent, respectively, displacements in the z and y directions. Model used: $2m=7+7$, $B_{\mathrm{LO}}=0.55$, $B_{\mathrm{TO}}=0.1$, $\omega_{\mathrm{LO}}^2-\omega_{\mathrm{TO}}^2=0.3$. The figures given in the upper right corners are the squared frequencies of the modes, with zero taken at ω_{LO}^2 (A).

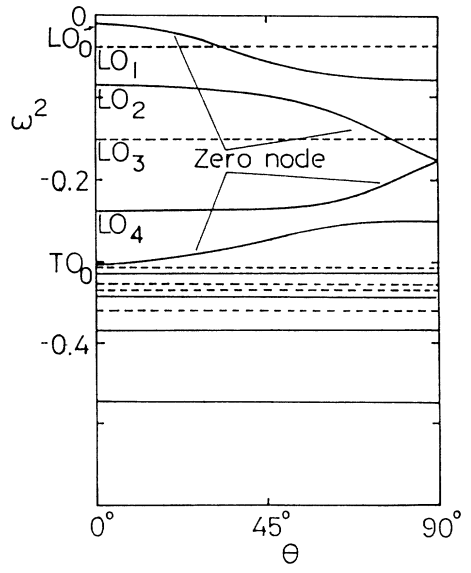

FIG. 2. The squared frequencies of long-wavelength modes as functions of the direction of propagation with the parameters taken to be the same as Fig. 1.

tions of direction of propagation θ. Out of the $4m=28$ modes, only the 14 modes confined to GaAs slabs are shown. The modes that remain unchanged owing to special symmetry are represented by dashed lines and the solid lines represent the modes changing with direction θ, though this is not apparent on the scale of the figure in many cases. We believe that the two branches which are observed to shift most conspicuously with θ [the shifted zero-node modes noted under (b) above] correspond to the "interface modes" in the dielectric theory, as suggested by Cardona.[8] Thus, like the "interface modes," these modes start off from the bulklike modes at $\theta=0°$, and at $\theta=90°$ we find that they show the typical variation with $d_1/(d_1+d_2)$ as discussed by Colvard *et al.*[2] (d_1 and d_2 are slab thicknesses of the two materials).

(d) Although our model is a special simplified model, with the incorporation of realistic material parameters, e.g., bulk material dispersion values for $\omega_{TO}(s),\omega_{LO}(s)$ (using the value for that material to which the calculated modes are mainly confined), the model yields realistic calculated results. Thus, as noted under (a) above, the calculated confined modes fall accurately on the bulk dispersion curves. The calculated results for another direction of propagation should be equally accurate, for the difference is only in the $s=0$ modes, which are precisely represented in the model in each case.

In conclusion, the above calculations demonstrate that all long-wavelength optic modes are generally dependent on the directions of propagation. Clearly the bulklike modes cannot be simply identified with modes of isolated slabs as in the dielectric theory. As regards the failure of the dielectric theory with respect to the bulklike modes, it may be noted that Sood *et al.* in their paper[5] apparently already noted a discrepancy between their experimentally observed LO modes and the vibration patterns predicted by a slab model treated as a dielectric continuum;[4] their experimental results agree with the results obtained above, namely, that the modes have nodes at the two faces of the confining layers.

This work was supported by the China National Natural Science Foundation.

---

*Also at the Department of Physics and Measurement Technology, Linköping University, Linköping, Sweden.

[1]S. M. Rytov, Zh. Eksp. Theor. Fiz. **29**, 605 (1955) [Sov. Phys.—JETP **2**, 466 (1956)].

[2]C. Colvard, T. A. Gant, M. V. Klein, R. Merlin, R. Fisher, H. Morkoç, and A. C. Gossard, Phys. Rev. B **31**, 2080 (1985).

[3]R. E. Camley and D. L. Mills, Phys. Rev. B **29**, 1695 (1984).

[4]R. Fuchs and K. L. Kliewer, Phys. Rev. **140**, A2076 (1965).

[5]A. K. Sood, J. Menendez, M. Cardona, and K. Ploog, Phys. Rev. Lett. **54**, 2111 (1985).

[6]J. E. Zucker, A. Pinczuk, D. S. Chelma, A. Gossard, and W. Wiegmann, Phys. Rev. Lett. **53**, 1280 (1984).

[7]M. V. Klein, IEEE J. Quantum Electron. **QE-22**, 1760 (1986).

[8]M. Cardona (private communication).